

***P-V* equation of State, thermal expansion, and *P-T* stability of synthetic zincochromite (ZnCr₂O₄ spinel)**

DAVIDE LEVY,¹ VALERIA DIELLA,² ALESSANDRO PAVESE,^{2,3,*} MONICA DAPIAGGI,²
AND ALESSANDRA SANI⁴

¹Dipartimento Scienze Mineralogiche e Petrologiche, Università degli Studi di Torino, Via Valperga Caluso 35, 10025 Torino, Italy

²National Research Council, IDPA, Milan section, Via Botticelli 23-20133 Milano, Italy

³Dipartimento Scienze della Terra, Università degli Studi di Milano, Via Botticelli 23-20133 Milano, Italy

⁴European Synchrotron Radiation Facility, ESRF-F 38043 Grenoble Cedex, France

ABSTRACT

The elastic properties and thermal behavior of synthetic zincochromite (ZnCr₂O₄) have been studied by combining room-temperature high-pressure (0.0001–21 GPa) synchrotron radiation powder diffraction data with high-temperature (298–1240 K) powder diffraction data. Elastic properties were obtained by fitting two Equations of State (EoS) to the *P-V* data. A third-order Birch-Murnaghan model, which provides results consistent with those from the Vinet EoS, yields: $K_0 = 183.1(\pm 3.5)$ GPa, $K' = 7.9(\pm 0.6)$, $K'' = -0.1278$ GPa⁻¹ (implied value), at $V_0 = 577.8221$ Å³ (fixed). Zincochromite does not exhibit order-disorder reactions at high temperature in the thermal range explored, in agreement with previous studies. The volume thermal expansion was modeled with $\alpha_V = \alpha_0 + \alpha_1 T + \alpha_2/T^2$, where only the first coefficient was found to be significant [$\alpha_0 = 23.0(4) \cdot 10^{-6}$ K⁻¹]. Above 23 GPa diffraction patterns hint at the onset of a phase transition; the high pressure phase is observed at approximately 30 GPa and exhibits orthorhombic symmetry. The elastic and thermal properties of zincochromite were then used to model by thermodynamic calculations the *P-T* stability field of ZnCr₂O₄ with respect to its oxide constituents (Cr₂O₃ and rocksalt-like ZnO). Spinel is expected to decompose into oxides at about 18 GPa and room temperature, in absence of sluggish kinetics.

INTRODUCTION

Spinel [ideally AB₂O₄, S.G: *Fd3m* Wells (1984); A and B usually divalent and trivalent cations, respectively] are ternary oxides widely studied for their high temperature (HT) A-B order-disorder reaction over tetrahedral and octahedral structural sites (see, for instance, Della Giusta et al. 1996 and Redfern et al. 1999; Sack 1982 for petrogenetic inferences). The behavior of spinels at high pressure (HP) has also recently attracted a great deal of interest (Levy et al. 2004, 2003, 2001; Funamori et al. 1998; Irifune et al. 1998; Yutani et al. 1997), as the spinel-like structure provides a model for phases stable under mantle conditions (ringwoodite). Spinel, moreover, exhibit pressure-induced phase transitions to CaM₂O₄-like structures, where M = Fe, Mn, and Ti (Dubrovinsky et al. 2003; Wang et al. 2002; Andrault and Bolfan-Casanova 2001; Levy et al. 2000; Fei et al. 1999; Irifune et al. 1991).

Zincochromite (ZnCr₂O₄) is a relatively poorly studied spinel in terms of HT and HP behavior (Catti et al. 1999; Wang et al. 2002), although it has been extensively investigated as a technological material by virtue of its magnetic (Kagomiya et al. 2004, 2002; Chen et al. 2002), electronic (Koga et al. 2004), and catalytic (El-Sharkawy 1998) properties. With this in mind, we undertook a study of synthetic ZnCr₂O₄ at high pressure (up to 44

GPa, by HP synchrotron radiation powder diffraction, with ID9A at ESRF) and high temperature (up to 1240 K, by HT laboratory X-ray powder diffraction) to determine the *P-V* and *T-V* Equations of State of zincochromite, and to investigate its stability as a function of *P* and *T*, by combining our results with those from earlier measurements and theoretical calculations. The present work also provides a contribution to the systematic study of the behavior of spinels at HP as a function of their composition. ZnCr₂O₄ lends itself well to comparison with franklinite (Levy et al. 2000) and gahnite (Levy et al. 2001) to rationalize the change of elastic properties as a consequence of chromium-iron and chromium-aluminum replacements, respectively.

EXPERIMENTAL METHODS

The ZnCr₂O₄ sample was synthesized by mixing and pressing into a pellet analytical purity ZnO and Cr₂O₃ reagent grade powders (Carlo Erba Reagenti) with an excess (≈ 1 wt%) of ZnO (O'Neill and Dollase 1994). The blend was heated at 1300 °C for 1 day, then cooled down to ambient temperature at an estimated rate of ≈ 20 –25 °/h. The remaining excess of zinc oxide was removed by washing the powder in dilute nitric acid, and then the full heating cycle and treatment were repeated. X-ray powder diffraction (laboratory X'PERT Philips diffractometer) showed no residual parent phases. Chemical analyses obtained from a polished epoxy mount of cemented powder using an Applied Research Laboratories SEMQ microprobe equipped with 6 wavelength-dispersive crystals and natural chromite and niccolite as standards for Cr and Zn, respectively, yielded the following composition: Zn_{0.97(6)}Cr_{2.02(4)}O₄. The uncertainties reported take into account the propagation of errors in averaging 15 analyses. Hereafter we use the ideal composition, i.e., ZnCr₂O₄, in place of the actual one, as such an approximation is fully consistent with the uncertainties observed and suffices for the purposes

* E-mail: alessandro.pavese@unimi.it

of the present investigation.

High-pressure powder-diffraction patterns were collected at beam-line ID9A of the European Synchrotron Radiation Facilities (ESRF, Grenoble, France), using a $<5\ \mu\text{m}$ grain size powder. Measurements were obtained from two experiments: (1) one up to 10 GPa, using a 600 μm culet Diamond Anvil Cell (DAC) and (2) the other up to 44 GPa, using a 300 μm culet DAC. In both cases we used N_2 as a pressure transmitting medium, and a steel gasket with a 125 μm diameter sample hole. P was determined by the shift of the fluorescence line of a ruby excited by an Ar laser, adopting the non-linear hydrostatic pressure scale of Mao et al. (1986). The ruby crystal was positioned in the HP cell so as to be in the centre of the incident X-ray beam. Equilibrium was assumed when the pressure measured every 10 minutes did not oscillate more than 0.01 GPa. The effects of a non-hydrostatic pressure distribution in the DAC were analyzed following the approach of Levy et al. (2004), based on Singh (1993) and Duffy et al. (1995). This method allows one to estimate the difference in terms of stress along the thrust axis (σ_3) and normal to it (σ_1). Calculated $\sigma_3 - \sigma_1$ values [using the elastic constants for MgAl_2O_4 from Askarpour et al. (1993), in the absence of data for zincochromite] ranged from -1.3 to 1.5 GPa, without a definite trend, with an average of about 0.03 GPa and a standard deviation of 0.5 GPa. We decided to use a nominal uncertainty of 0.1 GPa on P to fit the experimental P - V curve, according to our previous experience with data collected at ID9A under similar conditions. This was motivated by the fact that the uncertainties on the elastic constants of ZnCr_2O_4 might skew the inferred K_0 and K' values, had we used a weighted scheme based on $\sigma(P) = \sigma_3 - \sigma_1$ in the EoS calculations. Note that $\sigma(P) = 0.1$ GPa is likely an underestimation of the actual uncertainty, and therefore we expected P - V fittings giving χ^2 values significantly larger than unity. Measurements were carried out using an angle dispersive set up: a monochromatic beam ($\lambda = 0.41507\ \text{\AA}$, by Si-NBS calibration) was focused onto a $30 \times 30\ \mu\text{m}^2$ spot, and powder diffraction rings were recorded with a 2D imaging plate (MAAR345, with $100 \times 100\ \mu\text{m}$ pixel size) placed 359.935 mm from the sample. Such an experimental set up provides an angular resolution of about 0.04° and allows data collection times (recording, readout, and erasing) <1 – 2 min. The 2D diffraction rings were then converted into 1D 2θ -patterns using the FIT2D software (Hammersley et al. 1996). Saturated diffraction spots, erased before the 2D into 1D pattern transformation, occurred in the recorded images, presumably as a consequence of preferred orientation of crystallites in the HP cell. The GSAS-EXPGUI software (Larson and Von Dreele 2000; Toby 2001) was used for structure refinements. Crystalline N_2 was first taken into account by a multiphase refinement, but this approach did not work very well and we chose to manually cancel the contribution of crystalline N_2 at the image integration stage. The increasing overlap at HP between the diffraction signals of spinel and N_2 made it impossible to eliminate the contribution of the nitrogen peaks above 21 GPa. The quality of the collected powder patterns did not allow full structural refinements, and we had to restrict our analysis to the behavior of the cell edge of spinel as a function of P . In Figure 1a we show the powder diffraction pattern obtained at 6.4 GPa. Above 23 GPa, some spinel peaks exhibited an asymmetry which hampered the refinement of reliable lattice parameters. At about 29 GPa, shoulders appeared on the left of the main diffraction peaks of spinel. These shoulders developed into visible peaks which grew progressively in intensity with increasing P and, at about 40 GPa, the presence of a new phase became apparent, whereas spinel gave a modest contribution (Fig. 1b). We tried to fit the diffraction pattern of the new phase using the simple oxide constituents and the CaM_2O_4 -like structure models (Introduction). The diffraction patterns of oxides do not fit our observations, whereas those of the CaMO_4 -like structures provide a reasonable agreement, although no choice can be made between the different orthorhombic models [$Pmmn$ (Pausch and Müller-Buschbaum 1974); $Pnam$ (Becker and Kasper 1957); $Bbmm$ (Bertaut and Blum 1956); $Pbcm$ (Giesber et al. 2001); for a survey see Müller-Buschbaum (2003)].

Ambient pressure, high-temperature experiments were performed using an X'PERT Philips θ : θ diffractometer equipped with an AHT-PAP 1600 furnace. Optimal sample positioning throughout the accessible temperature range was achieved by means of a stepper motor which moves the sample downward as a function of the thermal expansion of the sample holder. The temperature is read on a thermocouple placed about 20 mm from the sample. Si-NBS was mixed with ZnCr_2O_4 powder as an inner calibrant to enhance the precision of the temperatures measured from the sample, and the thermal expansion of Swenson (1983) was used to determine T . Diffraction patterns were collected over the temperature range from 298 to 1240 K, between 17 and $118^\circ 2\theta$, with a step size of $0.02^\circ 2\theta$, a counting time of 4 s per step, and a heating rate of 25°min^{-1} . Before each HT data collection, the temperature was kept fixed for two hours to achieve thermal equilibrium. The data treatment was carried out by means of the GSAS-EXPGUI software. The quality of the HT measurements allowed us to perform full structure refinements.

RESULTS AND DISCUSSION

P - V equation of state

Table 1 reports the cell edge of ZnCr_2O_4 as a function of pressure. Two EoS models, shown below for the sake of completeness, were fitted to the observed P - V data: the Birch-Murnaghan EoS (Birch 1986) and the Vinet EoS (Vinet et al. 1986, 1987).

The Birch-Murnaghan EoS relies on a Taylor expansion of energy as a function of the Eulerian strain f_E and results in:

$$P(V) = 3K_0 f_E (1 + 2f_E)^{5/2} (1 + A f_E + B f_E^2) \quad (1)$$

TABLE 1. Cell edge of zincochromite as a function of P

1st experiment		2nd experiment	
P (GPa)	a (\AA)	P (GPa)	a (\AA)
0.0001	8.3291(7)	0.0001	8.3291(7)
0.33	8.32205(5)	1.97	8.29783(8)
1.13	8.31342(8)	4.67	8.26604(6)
1.87	8.30458(9)	7.15	8.2357(6)
3.31	8.28380(7)	8.69	8.2178(1)
4.22	8.26936(5)	9.66	8.2073(1)
4.94	8.26212(8)	11.28	8.1871(1)
5.86	8.2530(1)	12.9	8.17387(7)
6.44	8.2444(7)	13.56	8.16588(8)
7.84	8.2275(1)	14.67	8.1552(1)
8.63	8.2185(2)	15.79	8.1450(1)
9.74	8.2063(2)	17.65	8.1272(1)
		19.35	8.1178(2)
		21.04	8.1032(2)

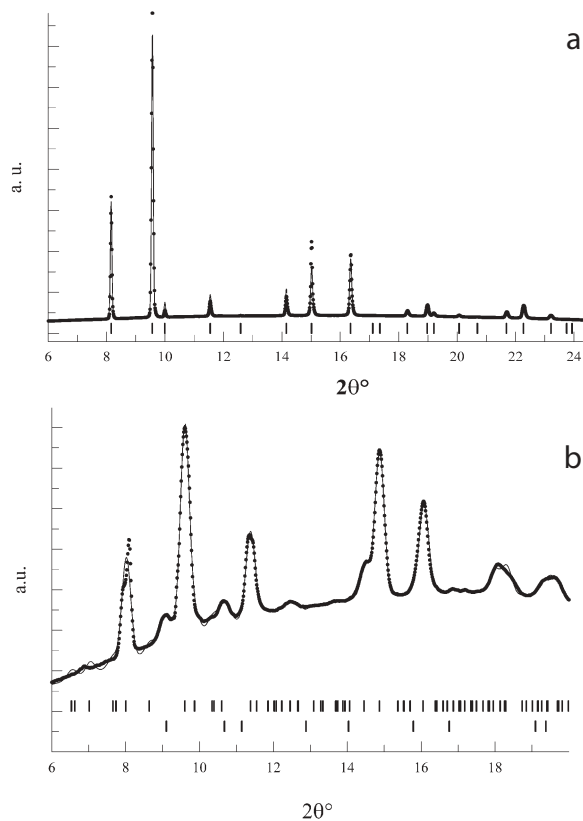


FIGURE 1. (a) Powder diffraction pattern at 6.4 GPa (bars are peak markers of spinel) and (b) at 44 GPa [upper and lower bars: peak markers of HP-phase (SG: $Pmmn$) and of spinel, respectively]. Dots are measurements, curves are fits.

where K_0 is the bulk modulus at $P = 0.0001$ GPa, $A = 3/2(K' - 4)$, and $B = 3/2[K_0K'' + (K' - 4)(K' - 3) + 35/9]$, with K' and K'' first and second pressure derivatives of bulk modulus at ambient conditions, respectively. f_E is defined as $f_E = [(V_0 / V)^{2/3} - 1]/2$ where V_0 and V are the volumes at $P = 0.0001$ GPa and at a given pressure, respectively.

The Vinet EoS, derived from quantum mechanics first principles, is:

$$P(V) = 3K_0 \frac{(1 - f_V)}{f_V^2} \exp[\eta(1 - f_V)] \quad (2)$$

where $\eta = 3/2(K' - 1)$ and $f_V = (V/V_0)^{1/3}$.

The best-fit parameters obtained by the EoS models reported above are given in Table 2; in Figure 2 the experimental P - V curve is displayed together with the calculations using the BM3 model. Figure 3, showing the normalized pressures as a function of the Eulerian strain, suggests that a third-order truncation of expansion (1) suffices to fit the experimental data, in agreement with most previous studies (see references in the introduction); this is consistent with the fact that BM4 and BM4V yield K' and K'' values $< 3\sigma$. The enhancement in terms of χ^2 -value provided by a fourth-order truncation is fictitious, and rather a consequence of an additional degree of freedom, than of a physically sound need for fitting K'' . The refinement of V_0 does not produce a significant decrease in χ^2 , and the resulting elastic parameters are in a general agreement with those from the fittings performed keeping V_0 at its experimental value. The confidence ellipses (Bass et al. 1981) displayed in Figure 4 show that BM3 and Vinet are

TABLE 2. Elastic parameters determined using different EoS models

EoS	V_0 (Å ³)	K_0 (GPa)	K'	K''_0 (GPa ⁻¹)	χ^2
BM3	577.8221	183.1(±3.5)	7.9(±0.6)	-0.1278	2.6
BM3V	578.0(3)	183.3(±5.1)	7.2(±0.5)	-0.1472	2.6
BM4	577.8221	198.1(±5.2)	1.7(±1.9)	0.75(±0.26)	1.9
BM4V	578.0(3)	207.3(±8.6)	-0.16(±2.4)	0.84(±0.30)	1.8
Vinet	577.8221	183.3(±2.2)	7.8(±0.4)		2.5
VinetV	578.0(3)	180.4(±4.7)	8.1(±0.6)		2.6

Notes: BM3 (third-order Birch-Murnaghan model), BM4 (fourth-order Birch-Murnaghan model), Vinet (Vinet model). Suffix V indicates that V_0 has also been refined. $\chi^2 = 1/N \sum_{j=1}^N (P_{\text{obs},j} - P_{\text{calc},j})^2 / \sigma(P)^2$. $\sigma(P) = \text{sqrt}(\sigma_P^2 + \sigma_V^2)$, where σ_P is the uncertainty on the experimental determination of P , and σ_V is the error on pressure calculated via EoS due to the propagation of the uncertainty on V .

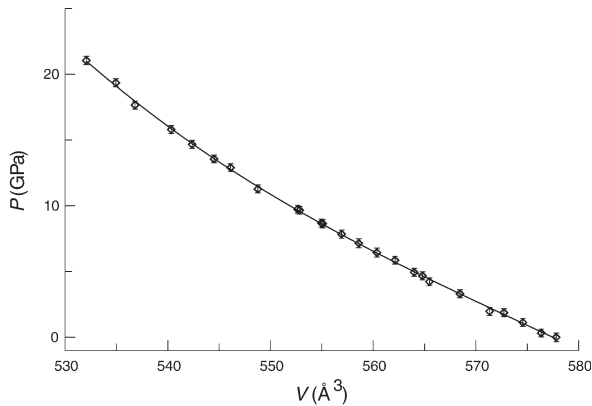


FIGURE 2. P - V curve. Empty diamonds are observed values; solid line represents the BM3 model (Table 2).

fully consistent with one another. In this light, we will henceforth use the BM3 model as a reference for our discussion.

Had we used $\sigma(P) = |\sigma_1 - \sigma_3|$, the third-order Birch-Murnaghan model would yield $K_0 = 188.7 \pm 1.3$ GPa and $K' = 6.3 \pm 0.2$, which are consistent within 2σ with the values of BM3 in Table 2.

The best-fit parameters of BM3 may be compared with the only previous determination of elastic properties for ZnCr₂O₄ in the literature, i.e., the quantum mechanics study of Catti et al. (1999), who provide K_0 and K' values of 215 GPa and 3.96 (Hartree-Fock model), and 285 GPa and 2.55 (Hartree-Fock model and a posteriori correction for correlation energy). The discrepancy between measured K_0 and its theoretical value is about 15%, in keeping with the average precision of the Hartree-Fock technique in reproducing the elastic properties of crystals.

Hazen and Yang (1999) proposed a model which allows one to predict elastic properties of spinels as a function of octahedral and tetrahedral cation-oxygen bond lengths, and of their compressibilities (β_{X-O}). In Table 3 we compare the experimental K_0 values of some spinels with those calculated by means of the model in question, using bond lengths and bond compressibilities reported by Hazen and Young (1999), Hazen and Finger (1982), and Menegazzo et al. (1997). The normal spinel structure ZnX₂O₄ series (X = Al, Cr, Fe) reveals consistence between the predicted dependence of K_0 on the octahedral bond length compressibility [$\beta_{Al-O} < \beta_{Cr-O} < \beta_{Fe-O}$] and the measured bulk modulus values [$K_0(\text{franklinite}) < K_0(\text{zincchromite}) < K_0(\text{gahnite})$]. ZnCr₂O₄ and ZnAl₂O₄ show agreement between measurements and calculations, whereas an 11% discrepancy occurs for ZnFe₂O₄. MgAl₂O₄ was modeled to have a larger K_0 than gahnite, in contrast with

TABLE 3. Observed and calculated [model of Hazen and Yang (1999)] K_0 values

spinel	K_0 (GPa)	K_0 (GPa)	Structure	Source
	observed	predicted		
ZnCr ₂ O ₄	183	190	N	Present work
ZnFe ₂ O ₄	166	187	N	Levy et al. (2000)
ZnAl ₂ O ₄	202	197	N	Levy et al. (2001)
MgAl ₂ O ₄	191	201	N	Levy et al. (2003)
MgFe ₂ O ₄	182	183	I	Levy et al. (2004)
Fe ₃ O ₄	222	184	I	Haavik et al. (2000)

Note: N and I stand for normal and inverse structure, respectively.

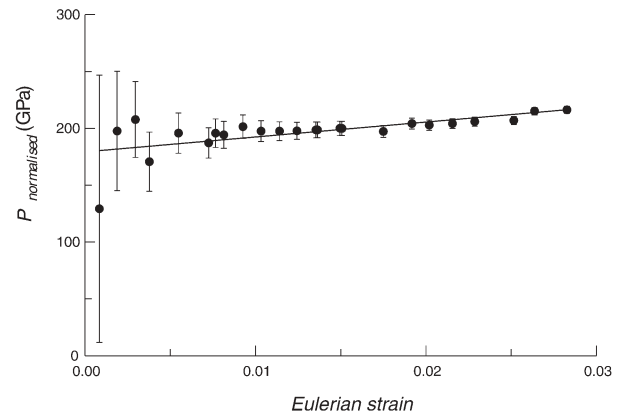


FIGURE 3. Normalized pressure $[= P / (3f_E(1 + 2f_E)^{5/2})]$ as a function of the Eulerian strain. Solid line is a linear fit.

the observations reported in Table 3. The K_0 value for MgAl_2O_4 might be reflective of the vacancies present in the sample used, as stated by Levy et al. (2003), causing an increase of the bond length compressibility. Note that an 8% change of the tetrahedral bond length compressibility suffices to shift the K_0 of MgAl_2O_4 in agreement with that measured. For MgFe_2O_4 , which is an Mg-Fe solid solution based on an inverse spinel structure, theoretical and experimental determinations of K_0 fully agree; this success makes us confident that the model of Hazen and Yang (1999) can be transferred to spinel solid solutions, though more experimental evidence is needed for a complete validation. Lastly, calculations and measurements are remarkably discrepant in the case of magnetite; however, one has to take into account that K_0 values earlier measured and reported by Haavik et al. (2000) cover a wide range (161–222 GPa).

Although the failure to fully refine the structure of ZnCr_2O_4 hampers a complete analysis of its behavior at HP, Levy et al. (2004, 2003) have observed that the one symmetry-independent coordinate (of oxygen) in spinels changes negligibly as a function of pressure, and the structural shrinking is mainly controlled by the cell-edge shortening. Given that the coordinate of oxygen in ZnCr_2O_4 shows a modest variation as a function of temperature (see the next section), one might expect a degree of “inertness” to P as well.

Thermal expansion

Table 4 reports the structural parameters refined as a function of temperature, up to about 1240 K. We did not carry out measurements above 1240 K for the following reasons: (1) a solid

TABLE 4. Cell edge, oxygen coordinate, and isotropic displacement parameters as a function of temperature

T (K)	a (Å)	x (oxygen)	$U_{\text{iso}}\text{O}$ (Å ²)	$U_{\text{iso}}\text{Cr}$ (Å ²)	$U_{\text{iso}}\text{Zn}$ (Å ²)	R_{wp}
298	8.3291(7)	0.2666(6)	8.3(2)	7.7(1)	7.9(1)	0.22
393	8.3330(7)	0.2666(6)	10.0(2)	9.6(1)	9.3(1)	0.27
463	8.3391(7)	0.2662(7)	10.1(2)	9.7(1)	9.7(1)	0.27
613	8.3456(7)	0.2665(6)	9.8(2)	9.6(1)	9.9(1)	0.28
702	8.3519(7)	0.2648(7)	10.2(2)	9.9(1)	10.2(1)	0.28
788	8.3588(7)	0.2642(8)	10.9(3)	10.1(1)	10.3(1)	0.27
901	8.3654(7)	0.2669(7)	10.7(3)	10.3(1)	10.5(1)	0.23
994	8.3716(7)	0.2648(7)	10.9(3)	10.2(1)	10.9(1)	0.27
1072	8.3777(7)	0.2675(6)	11.1(2)	10.5(1)	11.1(1)	0.26
1162	8.3834(7)	0.2676(6)	10.8(2)	10.5(1)	11.2(1)	0.25
1236	8.3880(7)	0.2650(8)	10.6(3)	10.6(1)	11.7(1)	0.23

Note: $R_{\text{wp}} = \sum w(I_{\text{obs}} - I_{\text{calc}})^2 / \sum w I_{\text{obs}}^2$, where w are statistical weights.

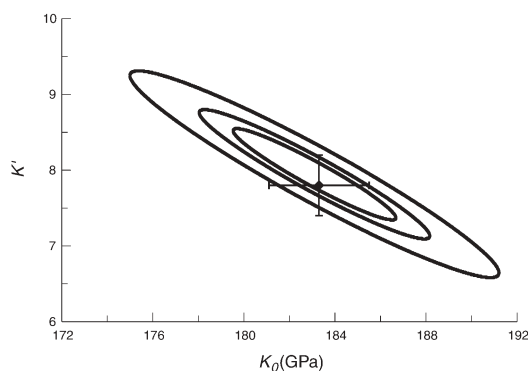


FIGURE 4. Confidence ellipses (68%, 90%, and 99%, from inner to outer, respectively). The elastic properties of the Vinet model correspond to the solid diamond.

state reaction involving zincochromite and Si takes place above 1200 K, with formation of eskolaite and willemite ($2\text{ZnCr}_2\text{O}_4 + \text{Si} + \text{O}_2 \rightarrow 2\text{Cr}_2\text{O}_3 + \text{Zn}_2\text{SiO}_4$); (2) the trend of the cell edge is quasi-linear, and we expect that points at higher temperatures would not add information significant to our aims. For the sake of brevity, we omit here the site occupancy factors, which have variations smaller than 3σ and confirm that the normal structure of ZnCr_2O_4 is a reliable approximation. The absence of change in the slope of the $a(T)$ curve (see Fig. 5), conversely observed in the case of MgFe_2O_4 at about 850 K (Levy et al. 2004) in relation to the onset of an order-disorder reaction, further suggests that no inversion occurs in the structure of ZnCr-spinel. Although the use of an approximate composition might hinder the occurrence of a very modest degree of inversion, our results are in full agreement with those of O'Neill and Dollase (1994), who reported no inversion in ZnCr_2O_4 after thermal treatment at 1300° C. All of this suggests that no order-disorder reaction relevant in terms of a configurational entropic contribution to stability has occurred. The volume thermal expansion is commonly modeled by (Fei 1995)

$$\alpha_V = \alpha_0 + \alpha_1 T + \alpha_2 / T^2 \quad (3)$$

The coefficients of Eq. 3 were determined by calculating the first temperature derivative of the curve $c + \alpha_0 T + 1/2\alpha_1 T^2 - \alpha_2/T$ fitted to the experimental $\ln[V(T)/V_0]$ values, where V_0 is the cell volume at room conditions. We observed that α_1 and $\alpha_2 < 1\sigma$; this motivated the use of a simpler expansion, i.e., $c + \alpha_0 T$, which yields $\alpha_0 = 23.0(4) \cdot 10^{-6} \text{K}^{-1}$. This value is comparable with those reported by Smyth et al. (2000) for MgAl_2O_4 , FeAl_2O_4 , and Fe_3O_4 , which range from 20.6 to $35.5 \cdot 10^{-6} \text{K}^{-1}$.

P-T field of stability

Because of the lack of thermodynamic data for the HP-phase, we have restricted our analysis of the ZnCr_2O_4 P - T field of stability (Fig. 6) to a comparison of spinel with its oxides (the rocksalt-like structures of ZnO and Cr_2O_3); the many approximations and assumptions we have made require due care in considering our inferences. The Gibbs energy of a phase is calculated by

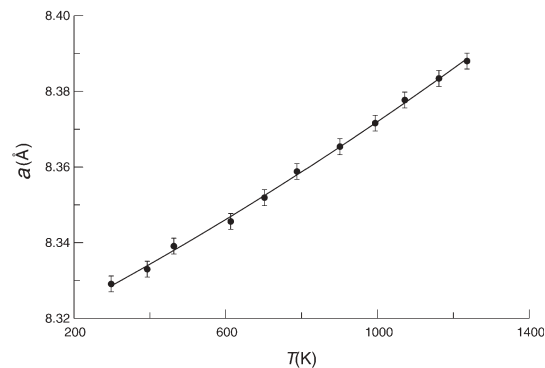


FIGURE 5. Cell edge as a function of temperature. Second order polynomial in T (solid line) to appreciate the smoothness of the experimental data.

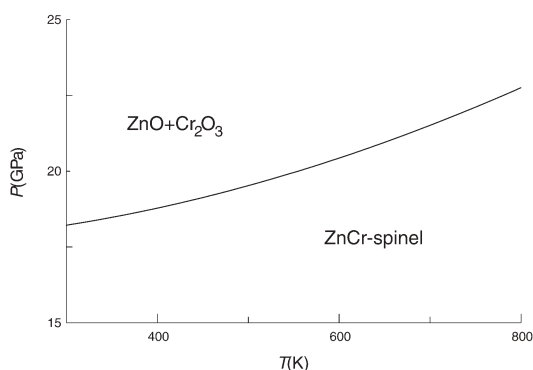


FIGURE 6. Calculated P - T field of stability of zincochromite and of its oxides.

$$E_B(0,0) + \int_{0,0}^{T,0} C_p(T')(1 - T/T')dT' + \int_{T,0}^{T,P} V(P',T)dP'$$

Experimental $E_B(0,0)$ [binding energy in the α -thermal limit at 0 K; values from Table 3 of Catti et al. (1999)] is available for Cr_2O_3 ; for ZnO and ZnCr_2O_4 we re-scaled the theoretical E_B s by the $E_B(\text{obs})/E_B(\text{calc})$ ratios computed for MnO and MgCr_2O_4 , respectively. $C_p(T) = C_v(T) + TV\alpha^2 / K$ (Wallace 1972), where specific heat at constant V is determined by the Debye model [where the Debye temperatures of ZnO , Cr_2O_3 , and ZnCr_2O_4 are replaced by those of wurtzite-like ZnO (Nedoseikina et al. 2000), Al_2O_3 (Goto et al. 1989), and ZnAl_2O_4 (Fang et al. 2002), respectively]. An experimental value for $C_p(T)$ [Klemme et al. (2000) and Klemme and Van Miltenburg (2004), for ZnCr_2O_4] would not change significantly our inferences in the T -range explored with respect to the approximations adopted. The thermo-elastic parameters reported here have been used for ZnCr_2O_4 ; for ZnO , $K_0 = 203$ GPa, $K' = 3.6$, $V_0 = 77.6 \text{ \AA}^3$ (Jaffe and Hess 1993), $\alpha_V = 5.2 \cdot 10^{-6} + 2.00 \cdot 10^{-8} T - 0.03 / T^2$ (Iwanaga et al. 2000, for wurtzite-like ZnO), and for Cr_2O_3 , $K_0 = 240$ GPa, $K' = 3.5$, $V_0 = 289 \text{ \AA}^3$ (Rekhi et al. 2000), $\alpha_V = 21.6 \cdot 10^{-6} + 0.11 \cdot 10^{-8} T - 0.29 / T^2$ (Fei 1995). Unavailable dK/dT values for ZnCr_2O_4 , ZnO and Cr_2O_3 have been replaced by those for MgAl_2O_4 , MgO , and Al_2O_3 , respectively (Anderson and Isaak 1995).

At room temperature, ZnCr -spinel is predicted to decompose into its oxides at about 18.3 GPa ($dP/dT \approx 0.014 \text{ GPaK}^{-1}$), in contrast with Catti et al. (1999) who indicate 34 GPa. Wang et al. (2002) determined the pressure of the phase transition (P_T) of zincochromite to an orthorhombic phase at about 17.5 GPa and room temperature, at variance with our experiment giving hints of onset of a structure transformation above 23 GPa. Significantly different experimental conditions can explain the discrepancy between the P_T of Wang et al. (2002) and ours (the absence of a pressure-transmitting medium leads to deviations from hydrostaticity and inhomogeneities of the stress field). In analogy with MgFe_2O_4 (Levy et al. 2004), ZnCr_2O_4 is expected to stabilize as a function of increasing P first as a spinel, then as oxides, and finally as an orthorhombic HP phase. Our failure in observing oxides and a fully defined HP phase, save above 30 GPa, is presumably due to sluggish transformations and want of peak resolution.

ACKNOWLEDGMENTS

The European Synchrotron Radiation Facility is kindly acknowledged for allocating beamtime for the measurements at high pressure and the National Research Council (CNR), Istituto per la Dinamica dei Processi Ambientali (IDPA), for the maintenance and functioning of the electron microprobe. The authors are grateful to W. van Westrenen and an anonymous referee for suggestions and corrections which enhanced the quality of the manuscript.

REFERENCES CITED

- Anderson, O.L. and Isaak, D.G. (1995) Elastic constants of mantle minerals at high temperature. In T.J. Ahrens, Ed., *Mineral Physics and Crystallography: A Handbook of Physical Constants*, 2, 64–97. American Geophysical Union, Washington, D.C.
- Andrault, D. and Bolfan-Casanova, N. (2001) High-pressure phase transformations in the MgFe_2O_4 and Fe_2O_3 - MgSiO_3 systems. *Physics and Chemistry of Minerals*, 28, 211–217.
- Askarpour, V., Manghnani, M.H., Fassbender, S., and Yoneda, A. (1993) Elasticity of single-crystal MgAl_2O_4 spinel up to 1273 K by Brillouin spectroscopy. *Physics and Chemistry of Minerals*, 19, 511–519.
- Bass, J.D., Liebermann, R.C., Weidner, D.J., and Finch, S.J. (1981) Elastic properties from acoustic and volume compression experiments. *Physics of the Earth and Planetary Interiors*, 25, 140–158.
- Becker, D.F. and Kasper, J.S. (1957) The structure of calcium ferrite. *Acta Crystallographica*, 10, 332–337.
- Bertaut, E.F. and Blum, P. (1956) Determination de la structure de Ti_2CaO_4 par la methode self-consistante d'approche directe. *Acta Crystallographica*, 9, 121–126.
- Birch, F. (1986) Equation of state and thermodynamic parameters on NaCl to 300 kbar in the high temperature domain. *Journal of Geophysical Research-Solid Earth*, 91, 4949–4954.
- Catti, M., Freyria Fava, F., Zicovich, C., and Dovesi, R. (1999) High-pressure decomposition of MCr_2O_4 spinels (M = Mg, Mn, Zn) by ab initio methods. *Physics and Chemistry of Minerals*, 26, 389–395.
- Chen, X.H., Zhang, H.T., Wang, C.H., Luo, X.G., and Li, P.H. (2002) Effect of particle size on magnetic properties of zinc chromite synthesized by sol-gel method. *Applied Physics Letters*, 81, 4419–4421.
- Della Giusta, A., Carbonin, S., and Ottonello, G. (1996) Temperature-dependent disorder in a natural $\text{Mg-Al-Fe}^{2+}\text{-Fe}^{3+}$ -spinel. *Mineralogical Magazine*, 60, 603–616.
- Dubrovinsky, L.S., Dubrovinskaia, N.A., McCammon, C., Rozenberg, G.K., Ahuja, R., Osorio-Guillen, J.M., Dmitriev, V., Weber, H.P., Le Bihan, T., and Johansson, B. (2003) The structure of the metallic high-pressure Fe_2O_4 polymorph: experimental and theoretical study. *Journal of Physics-Condensed Matter*, 15, 7697–7706.
- Duffy, T.S., Hemley, R.J., and Mao, H. (1995) Equation of state and shear strength at multimegabar pressures: magnesium oxide to 227 GPa. *Physical Review Letters*, 74, 1371–1374.
- El-Sharkawy, E.A. (1998) Textural, structural and catalytic properties of ZnCr_2O_4 - Al_2O_3 ternary solid catalysts. *Adsorption Science and Technology*, 16, 193–216.
- Fang, C.M., Loong, C.K., de Wijs, G.A., and de With, G. (2002) Phonon spectrum of ZnAl_2O_4 spinel from inelastic neutron scattering and first principles calculations. *Physical Review B*, 66, 14,4301–14,4307.
- Fei, Y.W. (1995) Thermal expansion. In T.J. Ahrens, Ed., *Mineral Physics and Crystallography: A Handbook of Physical Constants*, 2, 29–44. American Geophysical Union, Washington, D.C.
- Fei, Y.W., Frost, D.J., Mao, H.K., Prewitt, C.T., and Hausermann, D. (1999) In situ structure determination of the high-pressure phase of Fe_2O_4 . *American Mineralogist*, 84, 203–206.
- Funamori, N., Jeanloz, R., Nguyen, J.H., Kavner, A., Caldwell, W.A., Fujino, K., Miyajima, N., Shinmei, T., and Tomioka, N. (1998) High-pressure transformations in MgAl_2O_4 . *Journal of Geophysical Research-Solid Earth*, 103, 20813–20818.
- Giesber, H.G. III, Pennington, W.T., and Kolis, J.W. (2001) Redetermination of CaMn_2O_4 . *Acta Crystallographica C*, 57, 329–330.
- Goto, T., Yamamoto, S., Ohno, I., and Anderson, O.L. (1989) Elastic constants of corundum up to 1825 K. *Journal of Geophysical Research*, 94, 7588–7602.
- Haavik, C., Stølen, S., Fjellvåg, H., Hanfland, M., and Häusermann, D. (2000) Equation of state of magnetite and its high-pressure modification: thermodynamics of the Fe-O system at high pressure. *American Mineralogist*, 85, 514–523.
- Hammersley, A.P., Svensson, S.O., Hanfland, M., Fitch A.N., and Häusermann, D. (1996) Two-dimensional detector software: from real detector to idealised image or two-theta scan. *High Pressure Research*, 14, 235–248.
- Hazen, R.M. and Finger, L.W. (1982) *Comparative crystal chemistry*. Wiley, New York.
- Hazen, R.M. and Yang, H. (1999) Effects of cation substitution and order-disorder on P - V - T equations of state of cubic spinels. *American Mineralogist*, 84, 1956–1960.

- Irifune, T., Fujino, K., and Ohtani, E. (1991) A new high-pressure form of MgAl_2O_4 . *Nature*, 349, 409–411.
- Irifune, T., Nishiyama, N., Kuroda, K., Inoue, T., Isshiki, M., Utsumi, W., Funakoshi, K., Urakawa, S., Uchida, T., Katsura, T., and Ohtaka, O. (1998) The postspinel phase boundary in Mg_2SiO_4 determined by in situ X-ray diffraction. *Science*, 279, 1698–1700.
- Iwanaga, H., Kunishige, A., and Takeuchi, S. (2000) Anisotropic thermal expansion in wurtzite type crystals. *Journal of Materials Science*, 35, 2451–2454.
- Jaffe, J.E. and Hess, A.C. (1993) Hartree-Fock study of phase changes in ZnO at high pressure. *Physical Review B*, 48, 7903–7909.
- Kagomiya, I., Sawa, H., Siratori, K., Kohn, K., Toki, M., Hata, Y., and Kita, E. (2002) Structural phase transition and dielectric properties of ZnCr_2O_4 . *Ferroelectrics*, 268, 747–752.
- Kagomiya, I., Toki, M., Kohn, K., Hata, Y., Kita, E., and Siratori, K. (2004) Magnetic clusters in three dimensional spin frustrated system ZnCr_2O_4 . *Journal of Magnetism and Magnetic Materials*, 272–276 (Suppl. 1), 1031–1032.
- Klemme, S. and Miltenburg van, J.C. (2004) The entropy of zinc chromite (ZnCr_2O_4). *Mineralogical Magazine*, 68, 515–522.
- Klemme, S., O'Neill, H.St.C., Schnelle, W., and Gmelin, E. (2000) The heat capacity of MgCr_2O_4 , FeCr_2O_4 and Cr_2O_3 at low temperatures and derived thermodynamic properties. *American Mineralogist*, 85, 1686–1693.
- Koga, T., Nakatou, M., and Miura, N. (2004) Influence of thickness of oxide electrode on sensing performances of mixed-potential-type and impedancemetric NO_x sensors. *Chemical Sensors*, 20 (Suppl. A), 22–24.
- Larson, A.C. and Von Dreele, R.B. (2000) General Structure Analysis System (GSAS) Report LAUR, 748.
- Levy, D., Pavese, A., and Hanfland, M. (2000) Phase transition of synthetic zinc ferrite spinel (ZnFe_2O_4) at high pressure, from synchrotron X-ray powder diffraction. *Physics and Chemistry of Minerals*, 27, 638–644.
- Levy, D., Pavese, A., Sani, A., and Pischedda, V. (2001) Structure and compressibility of synthetic ZnAl_2O_4 (gahnite) under high-pressure conditions, from synchrotron X-ray powder diffraction. *Physics and Chemistry of Minerals*, 28, 612–618.
- Levy, D., Pavese, A., and Hanfland, M. (2003) Synthetic MgAl_2O_4 (spinel) at high-pressure conditions (0.0001–30 GPa): a synchrotron X-ray powder diffraction study. *American Mineralogist*, 88, 93–98.
- Levy, D., Diella, V., Dapiaggi, M., Sani, A., Gemmi, M., and Pavese, A. (2004) Equation of state, structural behavior and phase diagram of synthetic MgFe_2O_4 , as a function of pressure and temperature. *Physics and Chemistry of Minerals*, 31, 122–129.
- Mao, H.K., Xu, J., and Bell, P.M. (1986) Calibration of the ruby pressure gauge to 800 kbar under quasi-hydrostatic conditions. *Journal of Geophysical Research*, 91, 4673–4676.
- Menegazzo, G., Carbonin, S., and Della Giusta, A. (1997) Cation and vacancy distribution in an artificially oxidized natural spinel. *Mineralogical Magazine*, 61, 411–421.
- Müller-Buschbaum, H. (2003) The crystal chemistry of AM_2O_4 oxometallates. *Journal of Alloys and Compounds*, 349, 49–104.
- Nedoseikina, T.I., Shuvaev, A.T., and Vlasenko, V.G. (2000) X-ray absorption fine structure study on the anharmonic effective pair potential in ZnO and $\text{Zn}_{0.1}\text{Mg}_{0.9}\text{O}$. *Journal of Physics: Condensed Matter*, 12, 2877–2884.
- O'Neill, H.St.C. and Dollase, W.A. (1994) Crystal structures and cation distributions in simple spinels from powder XRD structural refinements: MgCr_2O_4 , ZnCr_2O_4 , Fe_3O_4 and the temperature dependence of the cation distribution in ZnAl_2O_4 . *Physics and Chemistry of Minerals*, 20, 541–555.
- Pausch, H. and Müller-Buschbaum, H. (1974) Die Kristallstruktur von $\alpha\text{-CaCr}_2\text{O}_4$. *Zeitschrift für Anorganische und Allgemeine Chemie*, 405, 113–118.
- Redfern, S.A.T., Harrison, R.J., O'Neill, H.St.C., and Wood, D.R.R. (1999) Thermodynamics and kinetics of cation ordering in MgAl_2O_4 spinel up to 1600 degrees C from in situ neutron diffraction. *American Mineralogist*, 84, 299–310.
- Rekhi, S., Dubrovinsky, L.S., Ahuja, R., Saxena, S., and Johansson, B. (2000) Experimental and theoretical investigations on eskolaite (Cr_2O_3) at high pressures. *Journal of Alloys and Compounds*, 302, 16–20.
- Sack, R.O. (1982) Spinel as petrogenetic indicators: activity composition relations at low pressures. *Contributions to Mineralogy and Petrology*, 79, 169–186.
- Singh, A.K. (1993) The lattice strains in a specimen (cubic system) compressed non-hydrostatically in an opposed anvil device. *Journal of Applied Physics*, 73, 4278–4286.
- Smyth, J.R., Jacobsen, S.D., and Hazen, R.M. (2000) Comparative crystal chemistry of dense oxide minerals. In R.M. Hazen and R.T. Downs, Eds., *High Temperature and high pressure crystal chemistry*, 41, 157–184. Review in *Mineralogy and Geochemistry*, Mineralogical Society and The Geochemical Society, Washington, D.C.
- Swenson, C.A. (1983) Recommended values for the thermal expansivity of silicon from 0 to 1000 K. *Journal of Physical and Chemical Reference Data*, 12, 179–182.
- Toby, B.H. (2001) EXPGUI, a graphical user interface for GSAS. *Journal of Applied Crystallography*, 34, 210–213.
- Vinet, P., Ferrante, J., Smith J.R., and Rose, J.H. (1986) A universal equation of state for solids. *Journal of Physics C: Solid State*, 19, L467–L473.
- Vinet, P., Smith, J.R., Ferrante, J., and Rose, J.H. (1987) Temperature effects on the universal equation of state of solids. *Physical Review B*, 35, 1945–1953.
- Wallace, D.C. (1972) *Thermodynamics of crystals*. Dover, Mineola, New York.
- Wang, Z., Lazor, P., Saxena, S.K., and Artioli, G. (2002) High pressure Raman spectroscopic study of spinel (ZnCr_2O_4). *Journal of Solid State Chemistry*, 165, 165–170.
- Wells, A.F. (1984) *Structural inorganic chemistry*. Oxford University Press, 5th ed., Oxford, U.K.
- Yutani, M., Yagi, T., Yusa, H., and Irifune, T. (1997) Compressibility of calcium ferrite-type MgAl_2O_4 . *Physics and Chemistry of Minerals*, 24, 340–344.

MANUSCRIPT RECEIVED JULY 1, 2004

MANUSCRIPT ACCEPTED NOVEMBER 24, 2004

MANUSCRIPT HANDLED BY JOHN AYERS